



Limiting slopes and depths at ebb-tidal shoals

Frank S. Buonaiuto^a, Nicholas C. Kraus^{b,*}

^a Marine Sciences Research Center, State University of New York at Stony Brook, Stony Brook, NY 11794, USA

^b US Army Engineer Research and Development Center, Coastal and Hydraulics Laboratory, 3909 Halls Ferry Road, Vicksburg, MS 39180-6199, USA

Received 19 November 2001; received in revised form 23 October 2002; accepted 15 November 2002

Abstract

Dense bathymetry surveys obtained by LIDAR at 13 small to medium coastal inlets of the continental United States were analyzed to quantify limiting (maximum) bottom slopes of ebb shoals and entrance channels. The LIDAR data were supplemented with conventional bathymetry measurements from five large inlets to obtain predictive relationships for the limiting (minimum) depth over crest of the ebb shoal. The sites, all located on sandy coasts, were chosen to cover a range in tidal amplitude, tidal prism, and average annual wave height. Wave-dominated inlets exhibited steeper slopes on their seaward margins than tide-dominated inlets. Slopes on ebb shoals typically do not exceed 4–6°, with seaward slopes being 1–2° steeper than landward slopes. Dredged entrance channels have steeper slopes than natural channels, with maximum slopes immediately after dredging reaching 6–8°. At one inlet having a series of LIDAR surveys, entrance channel maintenance dredging created 3–5° side slopes that decreased 0.5–1°/year for the next 2 years to achieve a typical slope of 3° along much of the channel. Greatest bottom slopes are found in scour holes near jetties (10–12°) and at the entrance bars (8–10°) of (tideless) Great Lakes harbors. Limiting depth over crest of the ebb shoals is predicted well by the parameter $(H_S P)^{1/4}$, where H_S is the average annual significant wave height, and P is the spring tidal prism. High correlation was also found between limiting depth and prism, and with limiting depth and wave height.

© 2002 Elsevier Science B.V. All rights reserved.

Keywords: Channels; Coastal inlets; Ebb-tidal shoals; Lidar; Limiting depth; Slopes

1. Introduction

The ebb shoal, channel, and related morphologic features at coastal inlets evolve under the action of the tidal current (or current associated with seiche on the Great Lakes of the United States), waves and wave-generated currents, and surrounding geologic framework. Storms, river flows, wind-generated currents, jetties, and dredging are other mechanisms and interventions

controlling inlet morphology. Development of the ebb shoal also depends on the slope of the inner shelf and asymmetry of the tidal wave at the particular site. Despite the complexity of the physical processes (FitzGerald, 1996; FitzGerald and FitzGerald, 1977), morphologic characteristics of inlets, such as minimum channel cross-sectional area and volume of the ebb shoal, have been successfully quantified in terms of just a few parameters of which tidal prism plays a leading role.

Empirical relations are available for estimating a large number of long-term average morphologic properties of coastal inlets (Table 1). Many of the relations presented in Table 1 pertain to inlets of the United

* Corresponding author. Fax: +1-601-634-2055.

E-mail address: nicholas.c.kraus@erdc.usace.army.mil (N.C. Kraus).

Table 1
Examples of empirical and theoretical equilibrium relationships for tidal inlet morphology

Author	Morphologic feature or relation	Relationship
LeConte (1905), O'Brien (1931, 1969), Johnson (1972); Riedel and Gourlay (1980), Hume and Herdendorf (1990), etc.	Minimum channel cross-sectional area, A_C (note: LeConte, Riedel and Gourlay, and Hume and Herdendorf consider the longshore transport rate magnitude)	$A_C = C_1 P^n$
Escoffier (1940)	Inlet cross-sectional area stability	Closure curve
Bruun and Gerritsen (1959, 1960)	Inlet stability, sand bypassing type	P/Q_g
Floyd (1968), Floyd and Druery (1976)	Minimum entrance bar (ebb shoal) depth vs. channel depth; bar distance offshore vs. channel depth	linear
Jarrett (1976)	Minimum channel cross-sectional area, with and without jetties	$A_C = C_2 P^n$
Walton and Adams (1976), Marino and Mehta (1987)	Equilibrium ebb shoal volume, V_E (note: separate relations according to wave climate)	$V_E = C_3 P^m$
Shigemura (1981)	Equilibrium throat width, W	$W = C_4 P^s$
Gibeaut and Davis (1993)	Equilibrium ebb shoal area, A_E	$A_E = C_5 P^k$
Kraus (1998)	Derivation of minimum channel cross-sectional area relation [note: includes longshore sediment transport rate in C_2	$A_C = C_2 P^n$
Carr de Betts and Mehta (2001)	Flood shoal area, A_F , and volume, V_F	$A_F = C_6 P^p$ $V_F = C_7 P^q$

P =tidal prism; A_C minimum cross-sectional area of inlet; A_E (A_F)=equilibrium horizontal area of ebb (flood) shoal; V_E (V_F)=equilibrium volume of ebb (flood) shoal; C =empirical or derived coefficient; k, m, n, p, q, s =empirical or derived powers; W =minimum width of inlet throat; Q_g =gross longshore transport in a year.

States, as studied here. Other relations have been found for inlet morphology, including several describing the tidal flats and channels of the Wadden Sea, The Netherlands (Eysink, 1990). Summaries of the Wadden Sea empirical relations are contained in Van Goor (2001) and Kragtwijk (2001).

Almost 100 years ago, Le Conte (1905) noted that the minimum cross-sectional area, A_C , of an inlet channel was related to the spring tidal prism P as a power function of the form:

$$A_C = C_1 P^n \quad (1)$$

where C_1 and n are empirical coefficients, and n has a value close to unity. The form of Eq. (1) has been verified, for example, by O'Brien (1931, 1969), Johnson (1972), and Jarrett (1976) for inlets in the United States; by Bruun and Gerritsen (1960), Renger and Partensky (1980), Eysink (1990), and Gerritsen et al. (1990) for inlets in Europe; by Riedel and Gourlay (1980) for inlets in Australia; and by Hume and Herdendorf (1990) for inlets in New Zealand.

Floyd (1968) and Floyd and Druery (1976) found a linear correlation between minimum or limiting water

depth over the entrance bar and the depth of the entrance channel of inlets in Australia and the United States. Shigemura (1981) gave a predictive relation similar to Eq. (1) for the minimum width of an unstructured (natural) inlet to the tidal prism. In a different approach, Vincent and Corson (1981) developed empirical relationships among geometric parameters such as minimum depth of the ebb shoal, minimum inlet width, and area of the ebb delta, not considering hydrodynamic forcing.

Walton and Adams (1976) showed that the equilibrium volume of the ebb shoal was also related to tidal prism by an equation similar in form to Eq. (1), which was further validated for inlets in Florida by Marino and Mehta (1987). Walton and Adams (1976) determined slightly different values of the empirical coefficients according to the wave energy as low, moderate, or high. Gibeaut and Davis (1993) related areas of ebb shoals of selected inlets in Florida to the tidal prism. Recently, Carr de Betts and Mehta (2001) showed that an equation of the form of Eq. (1) also describes the volume of the flood shoal for selected inlets on the east and west coasts of Florida.

Escoffier (1940, 1977) deduced the general behavior of the stability of inlet cross-sectional area in terms of a macro-scale parameter such as spring tidal prism or mean maximum velocity of the flow through the inlet, and Bruun and Gerritsen (1959, 1960) classified inlet sand bypassing by a parameter formed as the ratio of tidal prism divided by the (predominantly wave-induced) annual gross or total transport to the inlet. Kraus (1998) derived an expression in the form of Eq. (1) as a balance between the competing mechanisms of longshore transport and tidal flushing in a model compatible with concepts of Bruun and Gerritsen (1959, 1960).

In a more qualitative study, Hayes (1979) classified tidal inlet morphology graphically by the two parameters of mean significant wave height and mean tidal range. For the wave-dominated category (relatively large wave height for a particular tidal prism), flood-tidal shoals are well developed, and ebb-tidal shoals tend to be small. For tidally dominated inlets (relatively large tidal range for a particular wave height), ebb-tidal shoals are well developed, and the flood shoal is relatively small. Tidal range can be considered as a surrogate for tidal prism, if bay areas are comparable. For additional review, De Vriend (1996) covers the morphology of tidal inlets, includ-

ing properties of channels, spacing along barrier islands, and flood basin volume below mean sea level, and Hayes (1991) discusses integrative qualitative models.

The above studies indicate that tidal prism and mean wave height or wave energy determine a variety of long-term average properties of the morphology at inlets. The present study continues in this vein by expressing two other equilibrium properties of mature ebb shoals and channels in terms of these macro-scale forcing parameters. The geomorphic properties considered are limiting slopes of the ebb shoal and natural and dredged channels, and the minimum or limiting depth over the ebb shoal. Such relations are of interest to those involved with channel maintenance and mining of ebb shoals for sand bypassing. Also, limiting relations can serve as checks for numerical model simulations of tidal inlet morphology.

2. Procedure

2.1. Bathymetry data

High-resolution bathymetry data sets for 13 inlets located on the Atlantic, Gulf, and Great Lakes coasts

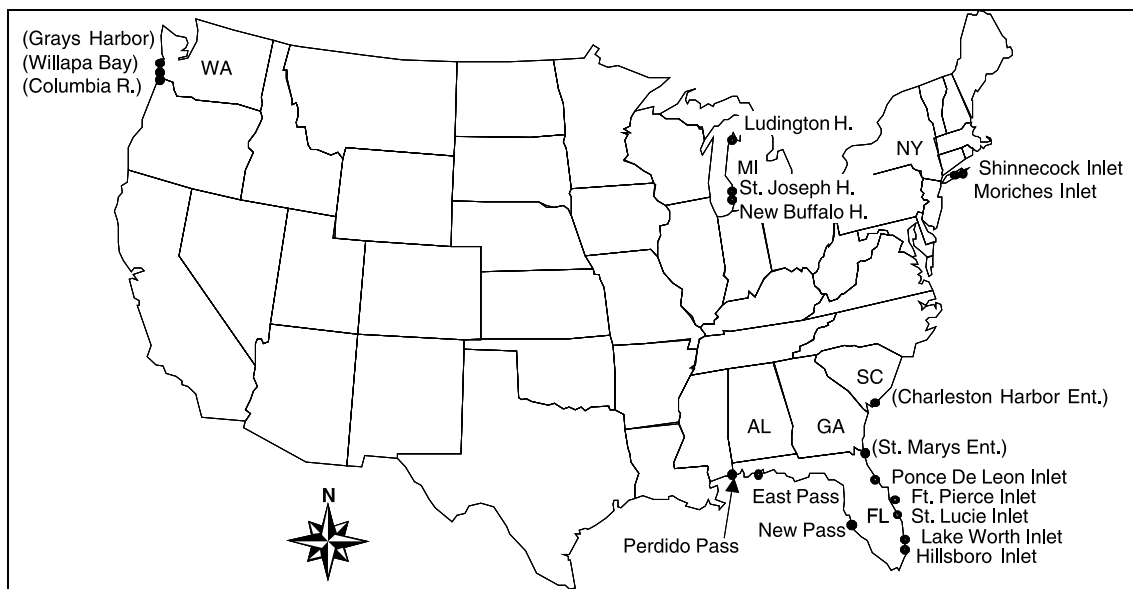


Fig. 1. Location of inlets examined (inlets with conventional surveys in parentheses).

of the United States (Fig. 1), some repeatedly surveyed (Table 2), were analyzed to determine spatial and temporal variability of limiting slopes and depths of ebb-tidal shoals and entrance channels. The Great Lakes sites served as an extreme case of no tide, although long-period lake seiching is present. These bathymetric surveys were collected by the US Army Corps of Engineers' Scanning Hydrographic Operational Airborne LIDAR Survey (SHOALS) system. The airborne-mounted system measures depth synoptically on flight swaths to a horizontal position accurate to 3 m and a vertical position accurate to 0.15 m (Parson et al., 1999). The maximum depth that SHOALS can survey is the shallower of either 60 m or about 2.5 times the Secchi Depth.

For analysis of depth over the ebb shoal, data sets from these inlets were supplemented by National Ocean Service (NOS) bathymetric soundings for Grays Harbor, Columbia River Entrance, and Willapa Bay entrance on the high-wave northwest coast of the United States; and from St. Mary's Entrance and

Charleston Harbor on the east coast of the United States. These locations extend the ranges in wave height and tidal prism. Conventional surveys from the six inlets are too sparse for analysis of channel slopes. Depths were adjusted to Mean Lower Low Water (MLLW), except for the Great Lakes harbors for which depths were converted to Mean Lake Level (MLL).

2.2. Wave and tidal prism information

The inlets analyzed vary between wave dominated and mixed-energy tide dominated (Hayes, 1979). Mean annual wave height ranges from 0.4 to 2.43 m and spring tidal range from 0 to 2.74 m, respectively (Table 3). For each inlet, the general wave climate in deep water was assembled from US Army Corps of Engineers' Wave Information Study (WIS) hindcasts (<http://www.bigfoot.wes.army.mil/w001.html>). For the Atlantic and Pacific Oceans, the statistical wave summaries are from the 20-year period 1976 through

Table 2
Survey information

Location	State	Date	Source	Tidal prism reference
Perdido Pass	AL	12/17/96	SHOALS	CIRP
		11/15/97	SHOALS	CIRP
East Pass	FL	12/29/96	SHOALS	Dombrowski (1994)
		10/25/97	SHOALS	
Fort Pierce Inlet	FL	5/(21–25)/95	SHOALS	Marino and Mehta (1987)
		5/18/97	SHOALS	
		10/17/97	SHOALS	
Hillsboro Inlet	FL	10/17/97	SHOALS	Jarrett (1976)
Lake Worth	FL	2/7/97	SHOALS	Dombrowski (1994)
New Pass	FL	9/94 12/94	SHOALS	Dombrowski (1994)
		11/28/95	SHOALS	
		9/(28–30)/96	SHOALS	
		11/(19–21)/97	SHOALS	
Ponce de Leon Inlet	FL	1/9/98	SHOALS	Jones and Mehta (1978)
St. Lucie Inlet	FL	2/(5–8)/97	SHOALS	Dombrowski (1994)
St. Mary's Entrance	GA	1979	NOS	Walton and Adams (1976)
Ludington Harbor	MI	7/31/97	SHOALS	
New Buffalo Harbor	MI	8/1/97	SHOALS	
St. Joseph	MI	8/4/97	SHOALS	
		6/23/98	SHOALS	
		5/22/96	SHOALS	CIRP
Moriches Inlet	NY	5/22/96	SHOALS	CIRP
Shinnecock Inlet	NY	8/13/97	SHOALS	Morang (1999)
		5/28/98	SHOALS	
Charleston Harbor	SC	1964	NOS	O'Brien (1969)
Columbia River	WA	1927	NOS	CIRP
Grays Harbor	WA	1955	NOS	Bruun and Gerritsen (1960)
Willapa Bay	WA	1927	NOS	Johnson (1972)

CIRP, Coastal Inlets Research Program (CIRP) database <http://www.cirp.wes.army.mil/cirp/cirp.html>.

Table 3
Inlet parameters and geomorphic classification

Location	State	H_s , m	Spring Tidal Range, m	Tidal prism, 10^6 m^3	h_c , m	Jetties	Hayes (1979) classification
Perdido Pass	AL	0.70	0.27	16.54	1.50	0	wave-dominated
		0.70	0.27	16.54		0	
East Pass	FL	0.60	0.15	15.17	2.50	2	wave-dominated
		0.60	0.15	15.17	2.25	2	
Fort Pierce Inlet	FL	0.80	0.94	17.30	4.00	2	mixed-energy wave-dominated
		0.80	0.94	17.30	4.00	2	
Hillsboro Inlet	FL	0.50	0.88		1.50	2	mixed-energy tide-dominated
Lake Worth	FL	1.00	0.94	28.40	5.50	2	mixed-energy wave-dominated
New Pass	FL	0.40	0.64	8.70	1.25	0	mixed-energy wave-dominated
		0.40	0.64	8.70	2.50	0	
		0.40	0.64	8.70	2.25	0	
		0.40	0.64	8.70	1.25	0	
Ponce de Leon Inlet	FL	0.40	0.82	16.25	2.50	2	mixed-energy tide-dominated
St. Lucie Inlet	FL	0.50	0.94	19.55	2.25	2	mixed-energy wave-dominated
St. Marys Entrance	GA	1.08	1.95	135.07	6.00	2	mixed-energy tide-dominated
Ludington Harbor	MI	0.70	0.00	0.00	3.25		wave-dominated
New Buffalo Harbor	MI	0.70	0.00	0.00	3.00		wave-dominated
St. Joseph	MI	0.79	0.00	0.00	2.75		wave-dominated
		0.79	0.00	0.00	3.25		
Moriches Inlet	NY	1.40	1.06	44.49	3.50	2	wave-dominated
Shinnecock Inlet	NY	1.20	1.06	33.20	2.50	2	wave-dominated
		1.20	1.06	33.20	2.50	2	
Charleston Harbor	SC	1.02	1.76	162.82	4.00	2	mixed-energy tide-dominated
Columbia River	WA	2.43	2.53	1100.00	10.00	2	mixed-energy wave-dominated
Grays Harbor	WA	2.35	2.74	521.00	10.00	2	mixed-energy wave-dominated
Willapa Bay	WA	2.35	2.46	490.00	8.00	0	mixed-energy wave-dominated

1995; for the Gulf of Mexico the 20-year period 1976 through 1995; and for the Great Lakes, the 32-year period 1956 through 1987. Tidal prisms were obtained from the literature and the US Army Corps of Engineers' Coastal Inlets Research Program database (<http://www.cirp.wes.army.mil/cirp/cirp.html>).

2.3. Sensitivity analysis

The spatial density of the data governs resolution of identifiable bathymetric features, but at the same time contamination of descriptions of larger scale forms by fine-scale bottom features such as ripples and ephemeral bars and troughs is to be avoided. Mean nearest-neighbor distances were calculated for each SHOALS data set. The overall mean distance between soundings of all SHOALS data was 4.6 m, with individual mean spacing ranging from 1.8 to 7.8 m. Data sets from Moriches Inlet and New Pass were analyzed by varying the grid interval and type

of interpolation procedure. Both inlets have similar morphology with a prominent ebb-tidal shoal, small bars residing on top of the shoals, and bisecting navigation channels. However, the soundings intervals for these inlets represent extremes in spacing in the SHOALS data set, with mean distances to the nearest neighbors of 3.1 m for Moriches and 7.6 m for New Pass. Questions can be raised as to whether a 3-m interval is too fine (introducing contamination by small features and artificial results through generation of numerical data points between measured points) and if a 7.6-m interval is too coarse (giving inadequate resolution of features of interest such as channel slopes). For calculating limiting slopes, sampling transects were constructed perpendicular to depth contours along the periphery of the ebb shoals and through the inlet channels, as illustrated in Fig. 2 for Moriches Inlet. Depths were mapped, and slopes were computed along each transect.

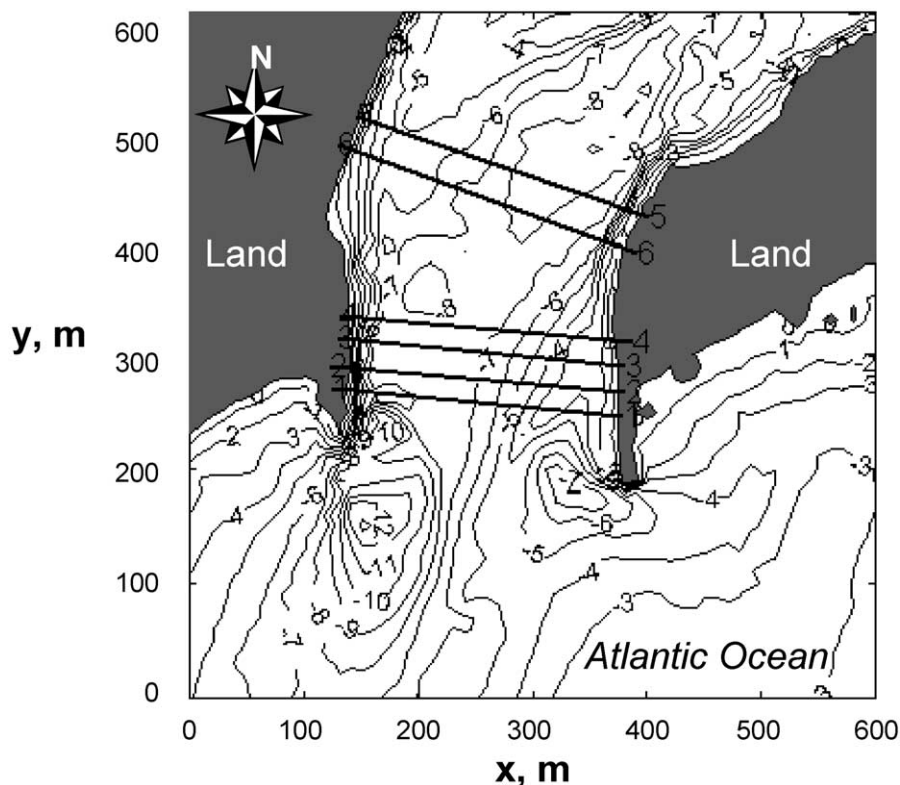


Fig. 2. Bathymetry contours and transect locations for Moriches Inlet, 1996 survey.

To quantify the influence of grid interval on calculated slopes and depths of ebb-shoal features, data from New Pass (1997) and Moriches Inlet (1996) were interpolated onto 3.048, 4.57, 7.62, 15.24, 22.86, and 30.48 m square grids. Contour plots and transects were constructed and analyzed for each interval selected. As expected, larger grid interval filtered (removed) small bedforms, giving a smoother representation of the bottom. Loss of information with larger sampling interval is illustrated in Fig. 3 for the 1997 Shinnecock Inlet survey (a survey with substantial spatial coverage), which shows the 1-m contours as produced from the six grid intervals listed above. In contrast, a smaller interval produced larger fluctuations in slope and bathymetric variations that appeared in contour maps as isolated promontories. Discrepancies between different grid intervals were most apparent in calculation of slopes along transects that bisected the lateral walls of the inlet channels. Here bathymetric change

that was poorly resolved (smoothed) by the larger grid spacing produced large scatter. Filtering of small bathymetric variations by the larger-spaced grids produced a smooth continuous contour plot, but this resolution reduced the accuracy of determined slopes and depths.

Sensitivity tests were performed to assess the variability of slope magnitude and its dependence on sample interval, Δx . The analysis compared several transects from regions with small bathymetric gradients (minimal morphologic variation). These regions, located up-drift and down-drift of the ebb shoal, were assumed to represent reliable measurements of the SHOALS uncontaminated by complex bottom features of various scales. The average deviation of transects from this ideal bathymetry was taken as an estimate of variability, which for these data sets ranged between 0.3 and 0.5°. Sensitivity of the variability estimates to grid spacing was examined by incrementing a decimated averaging-scheme along

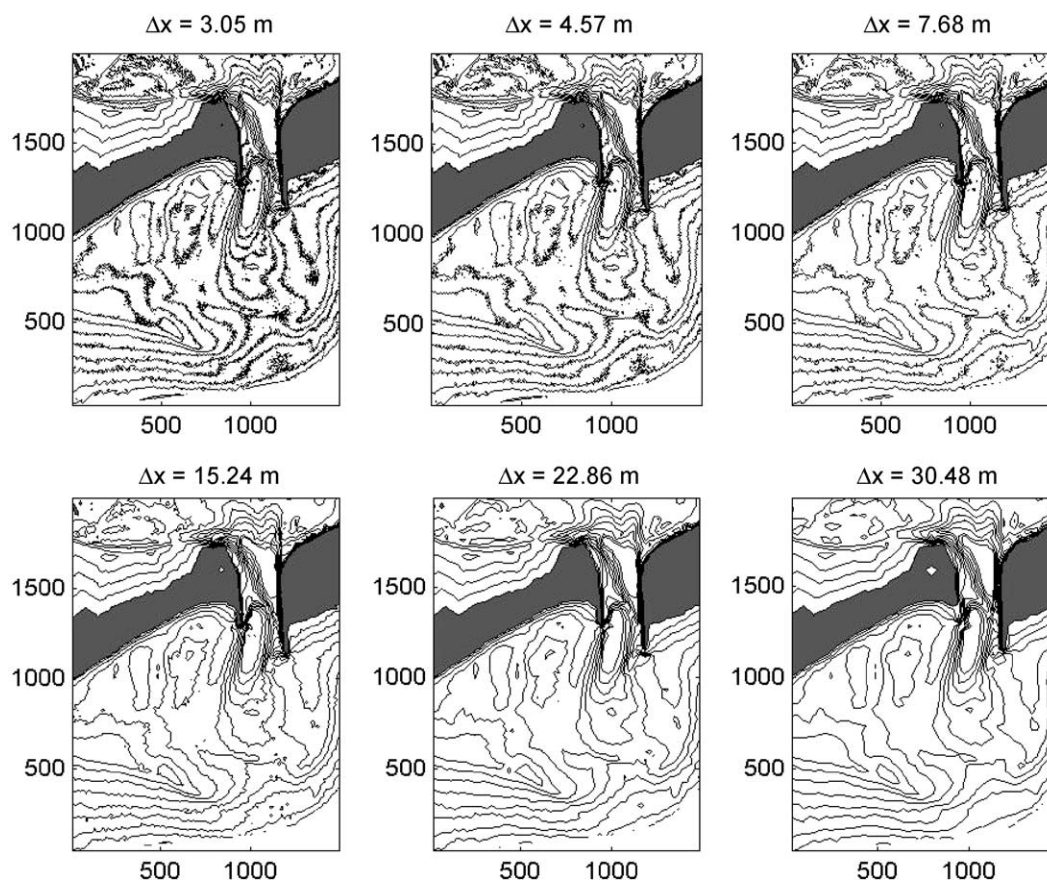


Fig. 3. Bathymetry contours drawn at 1 m interval for selected sampling intervals of the LIDAR data for Shinnecock Inlet, NY, survey of August, 1997.

each transect. Table 4 summarizes limiting slopes of channels and ebb shoals found for the evaluated grid intervals. Calculated slope magnitudes decrease uniformly with increased filtering from the largest interval of 100 m to the smallest of 5 m.

Based upon the mean sampling interval of all SHOALS data sets (4.6 m), more dense coverage through the inlet and around the ebb-tidal shoal, visual

inspection of contour maps, and sensitivity of calculated slopes to changes in interval, a 5-m square grid was judged to be optimal for this application. In addition to minimizing the amount of data lost to filtering, the 5-m interval resolved all significant features of the inlet identified by visual inspection of the original data without exaggerating isolated, smaller scale variations in the bathymetry.

Table 4
Slope dependence on grid spacing

Δx , m	Inlet channel slope, °	Ebb-shoal slope, °
5	8–10	4–5
25	6–8	2.5–3
50	5–7	2.25–3
100	3–5	1.75–2.5

3. Results

3.1. Limiting slopes

Steepest slopes were found at the shoreline, along the lateral sides of the inlet channels, sides of scour

holes, and around the seaward perimeter of the ebb-tidal lobe (Figs. 2–4). The distribution of slope magnitudes around the 1998 configuration of the ebb shoal at Shinnecock Inlet is displayed in Fig. 4, and Fig. 5 is a cross-section of the ebb shoal at this inlet that also illustrates notation. Typically, slopes on the ebb shoal and related bar features do not exceed 4–6°, and seaward slopes of the ebb shoal are 1–2° steeper than landward slopes. The lateral slopes associated with navigation channels shortly after dredging can be greater, with maximum values ranging from 6° to 8°. For natural channels, continual reworking of sediment by waves and tidal current smooths the bottom and reduces fluctuations, producing milder slopes that range from 3° to 5°. The channel slopes decrease seaward, with magnitudes varying between 1° and 2° on the outer ebb shoal. The largest gradients (steepest slopes) associated with the periphery of the ebb-tidal shoals were usually oriented

toward the predominant direction of the wave advance. Limiting (maximum) slopes that were computed from transects located in these regions ranged from 4° to 6°. Scour holes located near jetties contained the steepest slopes, ranging from 10° to 12° (Fig. 4).

Ebb shoals that experience higher waves were found to exhibit steeper slopes than those dominated by tidal forcing and with relatively smaller waves (Fig. 6). The linear regression relationship between the maximum slope observed on the ebb shoal and the significant wave height was ($R^2 = 0.75$):

$$\beta_{\text{ebb}} = 1.61 + 2.57H_S \quad (2)$$

where β_{ebb} is the limiting ebb-shoal slope in degrees, and H_S is the average-annual significant wave height in meters. Data sets collected after dredging across the ebb shoal (which temporarily creates steeper slopes)

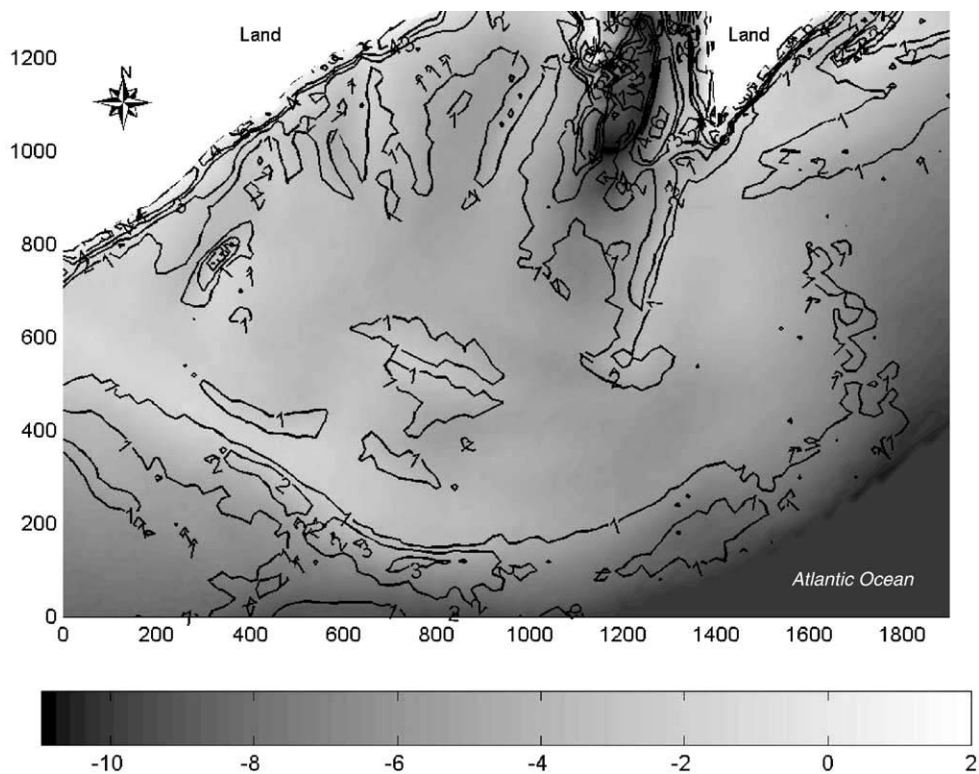


Fig. 4. Contours of slopes at Shinnecock Inlet ebb shoal, 1998 survey. Steepest regions are located along the lateral walls of the inlet channels, around the periphery of the ebb shoal, and along the shoreline.

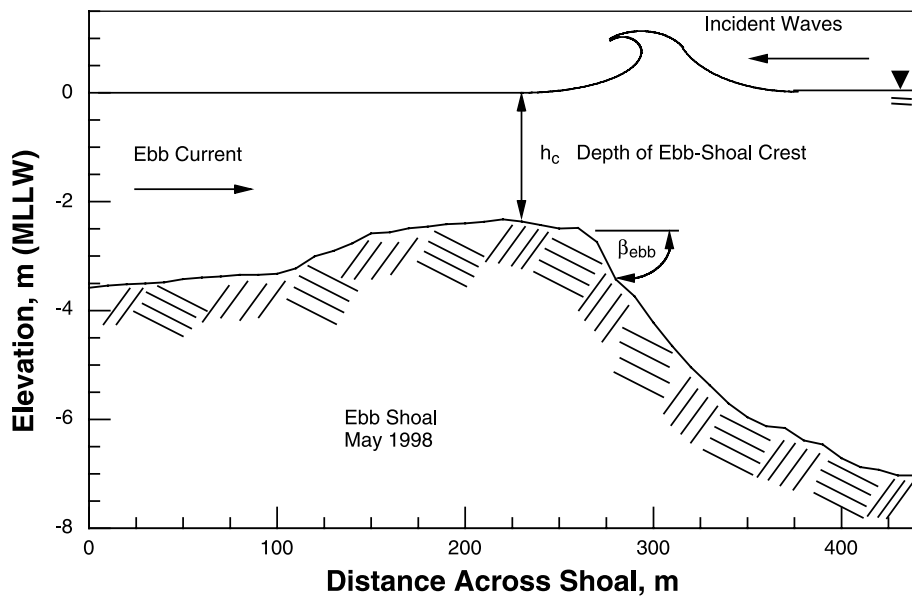


Fig. 5. Definition sketch for the depth over crest of an ebb shoal (cross-section from Shinnecock Inlet, NY, survey of May 1998).

were not included in the regression. Tidal prism, wave steepness, and combined tidal prism and wave height were also examined for predictive skill, but no correlation was found with limiting slope. Other factors

determining limiting bottom slopes are expected to include jetty configuration and sediment grain size.

Stabilized inlets such as Shinnecock Inlet and Moriches Inlet that have significant tidal forcing

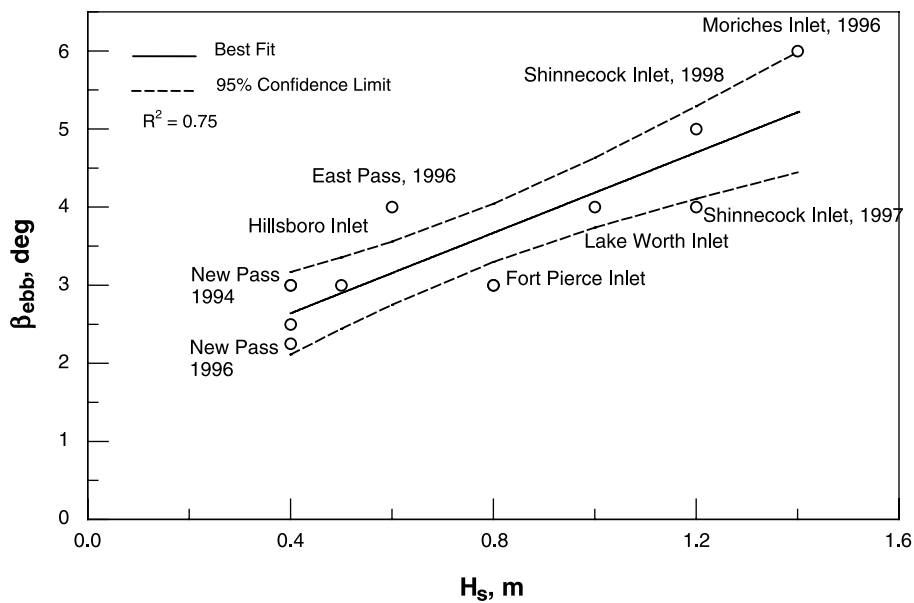


Fig. 6. Linear regression between the maximum slope observed on the ebb shoal and significant wave height.

through relatively narrow entrances maintain steeper channel slopes than the unstabilized inlets (New Pass and Perdido Pass, Table 3). Stabilization of an inlet with jetties confines the ebb-tidal jet and increases scour in the channel, whereas ebb flow at non-jettied inlets spreads through a larger cross-section, tending to smooth the bottom and creating favorable conditions for multiple shallow entrance channels. Although Moriches and Shinnecock Inlets receive significant wave forcing, wave action is not believed to control the slopes of the channel walls. In contrast, in areas where wave action dominates transport by tidal currents, both inlets have steep slopes along the ebb shoal, bypassing bar, and the attachment bar (Fig. 7)—morphologic features forming the inlet sand bypassing system (Kraus, 2000). The other inlets surveyed by the SHOALS system experience milder wave conditions than Shinnecock and Moriches Inlets, and these inlets exhibit more gently sloping ebb shoals and bypassing bars. Slopes along the down-drift attachment bars ranged from 1° to 4° for higher wave-energy inlets and 1° to 2° for lower wave regimes. Bar slopes become steeper as one moves from the attachment bar to the main ebb shoal.

Dredging alters the side slopes of channels. The entrance channel at New Pass was realigned perpendicular to the shoreline in 1991, and immediately began migrating to the down-drift southerly orientation (McClung and Douglass, 1999). In 1994, channel slopes at New Pass were on the order of $3\text{--}5^\circ$, and subsequent surveys showed that these slopes decreased by $0.5\text{--}1^\circ/\text{year}$. By 1996, the maximum slope in the southward migrating channel was about 3° . The initial realigned navigation channel through

the ebb shoal was again dredged in August 1997, and slopes on the order of 6° were observed 3 months later during the November survey. Slopes of the relict south-facing channel were greatest (2°) where it intersected the newly dredged channel. Maximum slopes along the seaward portion of the relict channel were 0.5° . The deflation of the relict channel walls on the outer shoal suggests that infilling processes are wave dominated and operate on those regions of the relict channel that experience the strongest wave forcing. By April 1998, the relict channel had filled with sand, and overlying bar features appeared to control the slopes along the down-drift portion of the ebb shoal. The seaward-most section of the main navigation channel showed signs of reworking as side slopes there decreased from 4° to 2° during the 8-month interval after dredging.

Four of the SHOALS-surveyed inlets (Shinnecock, Moriches, New Pass, and Lake Worth) showed asymmetries in side slopes of their cross-channel profiles. Near the throat, the asymmetries associated with steeper, up-drift channel slopes appear to be related to the encroachment by submerged spits or migrating shoals having slopes ranging from 1° to 3° . However, on the outer shoal the asymmetry in channel side slope, which may be on the order of $2\text{--}3^\circ$, will shift from up- to down-drift sides of the channel depending on the orientation of the channel.

The Great Lakes sites are representative of a different hydrodynamic regime, selected to provide the extreme situation of no tide. Without tide, the location of the surf zone varies through a smaller range, and waves break in a more confined area. Although some seiching occurs on the Great Lakes, morphology at its harbor entrances is predominantly controlled by waves, as evidenced by a continuous longshore bar observed in the data sets. Slopes along bar complexes at Great Lakes harbor entrances were substantially larger than at tidal coasts, ranging from 4° to 6° . In several locations slopes reached maximum values of $8\text{--}10^\circ$.

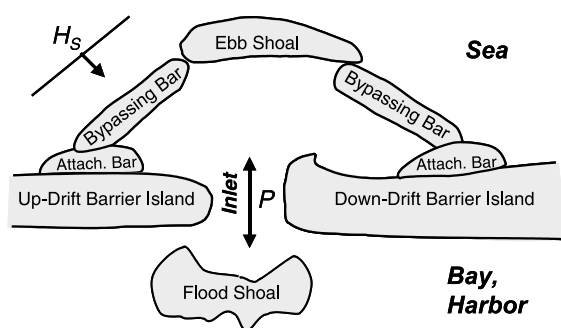


Fig. 7. Definition sketch for inlet morphology.

3.2. Depth over crest of ebb shoal

The bathymetric data enabled identification of ebb-shoal crests at all the inlets. The crest is defined as the shallowest water located directly seaward of the main ebb channel (Fig. 5). The shoal depth was

referenced to MLLW because it frequently is the controlling depth for wave propagation. The ebb jet is opposed by the incident waves, which can create breaking bars. Therefore, the limiting depth over the crest of the ebb shoal is expected to depend on both the tidal prism and wave height as main forcing parameters. The depth over crest and will also depend on geomorphologic factors such as grain size and sediment availability, inter-annual changes in the hydrodynamic forcing, and other factors not discussed here.

At Moriches Inlet, along the Long Island, NY, Atlantic coast and where the average annual wave height is 1.4 m and tidal prism $3.48 \times 10^6 \text{ m}^3$, the limiting depth over the crest of the ebb shoal is 3.5 m MLLW. New Pass is located on the west coast of Florida, with mild wave climate and small tidal range. The ebb shoal exhibits temporal variability, oscillating between limiting depths of approximately 1.25 and 2.5 m MLLW from 1994 through 1997. To resolve the depth of the ebb-shoal crest across the range of wave heights, the SHOALS data sets (collected at low and medium wave energy coasts) were supplemented with NOS data sets for Grays Harbor, Columbia River Entrance, and Willapa Bay

to expand the data range to higher energy inlets (Table 2). Grays Harbor, Willapa Bay, and the Columbia River have large tidal prisms and experience large waves. Charleston Harbor has a relatively large tidal prism, but experiences small waves as compared to the other larger inlets and entrances examined.

Interpretation of the depth over the ebb-shoal crest on transects was verified by surface-area computation, with each grid point representing 25 m^2 at 5-m spacing. The greater the surface area occupied by a particular depth of the ebb shoal, the more accurate the measurement. Analysis of the tidal inlet data revealed several functional relationships between the depth over the ebb-shoal crest and the tidal prism and average annual significant wave height.

Limiting (minimum) depth over ebb shoal crest was linearly regressed against the average annual significant wave height (Fig. 8), resulting in the predictive equation:

$$h_C = 0.27 + 3.6H_S \quad (\text{MLLW}) \quad (3)$$

where h_C is the depth over the ebb-shoal crest in meters relative to MLLW, and H_S is the average-

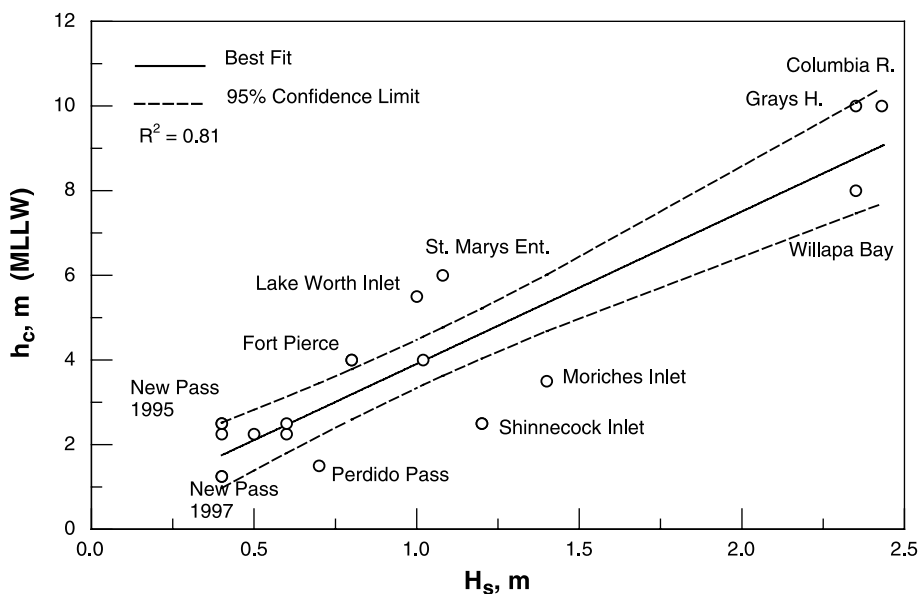


Fig. 8. Linear regression between the depth over crest of an ebb shoal and average-annual significant wave height.

annual deepwater significant wave height (m). The factor of 3.6 in front of the wave height in Eq. (3) for ebb shoals is much larger than that for the depth over crest for depth-limited waves breaking on longshore bars (which is 0.66; see Larson and Kraus, 1989) because of the erosion by the ebb jet. Although Eq. (3) predicts depth over the crest of the main ebb shoal with reasonable reliability ($R^2=0.81$), estimates for six data points fall outside of the 95% confidence intervals. Also, the relatively large constant or intercept, 0.27 m, suggests that a pertinent governing process is omitted, such as the tidal prism.

The seaward extent of the ebb shoal is known to depend on the tidal prism P (Floyd, 1968), so the depth over ebb-shoal crest was regressed with a power-law form similar to those listed in Table 1, namely $h_C = CP^n$, giving:

$$h_C = 0.0063P^{0.35} \quad (\text{MLLW}) \quad (4)$$

with $R^2=0.83$, but with eight data points lying outside the 95% confidence limits (Fig. 9). Eq. (4) is not convenient because of the awkward dimensional empirical coefficient.

Because the limiting depth over an ebb shoal is controlled by both wave height and tidal prism, a combination of those two quantities might have greater predictive power. For this purpose, the parameter $(H_S P)^{1/4}$ is introduced that has units of length (m). Regression with an assumed linear dependence yields:

$$h_C = -0.066 + 0.046(H_S P)^{1/4} \quad (\text{MLLW}) \quad (5)$$

which has an intercept of -0.066 m that is considerably less than the uncertainty in individual depth soundings, and Eq. (5) is convenient in having homogeneous units. Six data points remain outside of the confidence limits (Fig. 10), and the bands are tighter to the regression line ($R^2=0.87$) than in Figs. 8 and 9.

The three regression equations account for the variance in the data set reasonably well. The depth to the ebb-shoal crest was marginally better predicted by the combination of the incident wave height and tidal prism (Fig. 10), based upon R^2 values and cluster within the 95% confidence limits. Homogeneous units and scaled magnitude (reasonable magnitude of values) of the parameter $(H_S P)^{1/4}$ make it convenient for calculations.

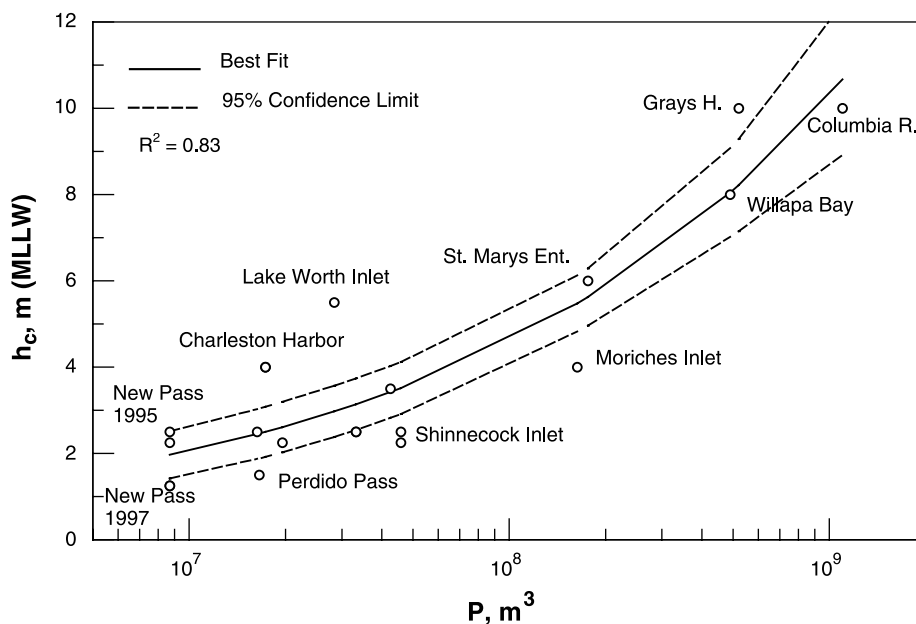


Fig. 9. Power law regression between the depth over crest of an ebb shoal and tidal prism.

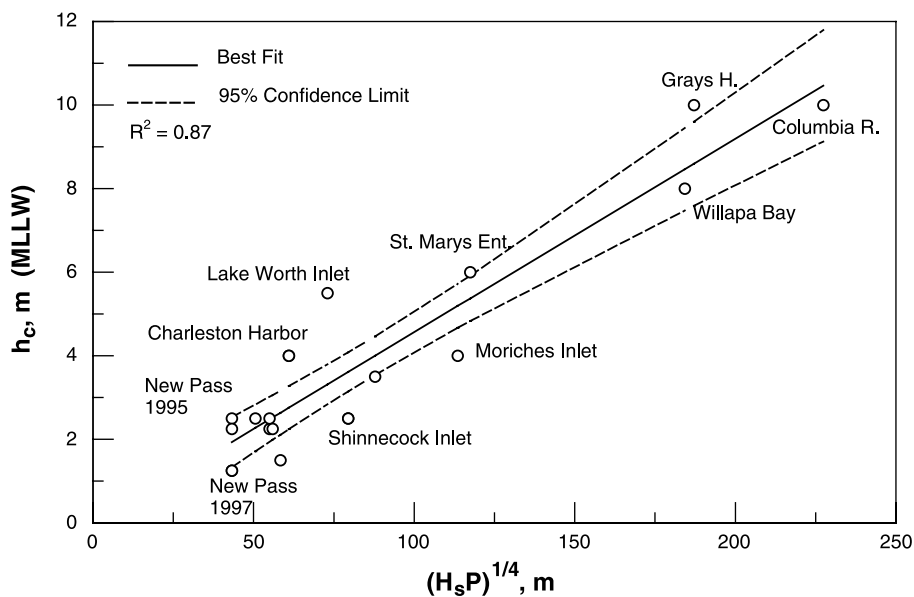


Fig. 10. Linear regression between the depth over crest of an ebb shoal and the product of significant wave height and tidal prism as $(H_S P)^{1/4}$.

As a final consideration, because Eq. (5) has a small intercept, a power law fit with the quantity $H_S P$ was performed to yield:

$$h_C = 0.0424(H_S P)^{0.254} \quad (\text{MLLW}) \quad (6)$$

which had a relatively high $R^2 = 0.87$, but with seven data points lying outside the 95% confidence limits. The exponent value of 0.254 in Eq. (6) indicates that the intuitively developed parameter $(H_S P)^{1/4}$ having units of length appears to possess physical significance that should be explored in future work.

4. Concluding discussion

Bathymetry data collected by the SHOALS system comprise a highly accurate and valuable source of synoptic information on bottom slopes and geometry of inlet morphologic features. At inlet entrances, steepest slopes are located along the shoreline, in scour holes, around the seaward margin of the ebb shoal, and along the lateral walls of navigation channels. Slopes recently dredged entrance channels ranged from 6° to 8° , with stabilized inlets sustaining greater slopes than unstabilized inlets. Maximum

slopes along the ebb shoal, occurring on the seaward periphery, are on the order of 4° . Wave-dominated environments sustain steeper slopes than tidally dominated regimes.

Almost equal predictive capability among the equations involving wave height only, tidal prism only, and the product of wave height and tidal prism may be an outcome of a data set that is predominantly composed of mixed energy inlets. For inlets that are mainly tide dominated, predictive power of the tidal prism may be greater than wave height for estimating depth over the ebb crest. However, it is difficult to define a unique ebb shoal crest for the complex shoals, such as channel margin bars, associated with tidally dominated inlets. For the analyzed data set, the limiting depth over an ebb-tidal shoal measured with respect to MLLW is best described by a quantity formed of the incident wave height and tidal prism as $(H_S P)^{1/4}$.

The empirically obtained relationships found here describe basic macro-morphological properties of ebb-tidal shoals and entrance channels. In addition to being of interest for characterizing morphological properties, such relationships are also expected to guide simulation of the evolution of inlet morphology by means of process-based numerical models.

Acknowledgements

This work was made possible through assistance of Mses. Jennifer Irish and Jennifer McClung of the Joint Airborne Lidar Bathymetry Technical Center of Expertise, US Army Corps of Engineers (USACE), Mobile District (<http://www.shoals.sam.usace.army.mil>) in providing the SHOALS data. This paper benefited from reviews by Dr. Duncan FitzGerald, Dr. Donald Stauble, and Ms. Shelley Johnston. This paper was prepared as an activity of the Inlet Geomorphology and Channels Work Unit, Coastal Inlets Research Program, USACE. Permission was granted by the Chief of Engineers, USACE, to publish this information.

References

- Bruun, P., Gerritsen, F., 1959. Natural bypassing of sand at coastal inlets. *J. Waterw. Harb. Div.*, ASCE 85 (4), 75–107.
- Bruun, P., Gerritsen, F., 1960. Stability of Tidal Inlets. North Holland, Amsterdam. 123 pp.
- Carr de Betts, E.E., Mehta, A.J., 2001. An assessment of inlet flood deltas in Florida. *Proc. Coastal Dynamics 01*, ASCE, 252–262.
- De Vriend, H.J., 1996. Mathematical modeling of meso-tidal barrier island coasts, Part I: empirical and semi-empirical models. In: Liu, P.L.-F. (Ed.), *Adv. Coast. Ocean Eng.*, vol. 2. World Scientific, River Edge, NJ, pp. 115–149.
- Dombrowski, M.R., 1994. Ebb tidal delta evolution and navigability in the vicinity of coastal inlets. UFL/COEL-94/010, Coastal and Oceanographic Eng. Dept., Univ. of Florida, Gainesville, FL. 96 pp.
- Escoffier, F.F., 1940. The stability of tidal inlets. *Shore Beach* 8 (4), 114–115.
- Escoffier, F.F., 1977. Hydraulics and stability of tidal inlets. GITI Rep., vol. 13. US Army Corps of Engineers, Coastal Eng. Res. Center, Vicksburg, MS.
- Eysink, W.D., 1990. Morphologic response of tidal basin to changes. *Proc. 22nd Coastal Eng. Conf.*, ASCE, 1948–1961.
- FitzGerald, D.M., 1996. Geomorphic variability and morphologic and sedimentologic controls on tidal inlets. *J. Coast. Res.*, Spec. Issue 23, 47–71.
- FitzGerald, D.M., FitzGerald, S.A., 1977. Factors influencing tidal inlet geometry. *Proc. Coastal Sediments '77*, ASCE, 563–581.
- Floyd, C.D., 1968. River mouth training in New South Wales. *Proc. 11th Coastal Eng. Conf.*, ASCE, 1267–1281.
- Floyd, C.D., Druery, B.M., 1976. Results of river mouth training on the Clarence Bar, New South Wales, Australia. *Proc. 15th Coastal Eng. Conf.*, ASCE, 1738–1755.
- Gerritsen, F., de Jong, H., Langerak, A., 1990. Cross-sectional stability of estuary channels in The Netherlands. *Proc. 22nd Coastal Eng. Conf.*, ASCE, 2922–2935.
- Gibeaut, J.C., Davis Jr., R.A., 1993. Statistical geomorphic classification of ebb-tidal deltas along the west-central Florida coast. *J. Coastal Res.*, Spec. Issue 18, 165–184.
- Hayes, M.O., 1979. Barrier island morphology as a function of tidal and wave regime. In: Leatherman, S.P. (Ed.), *Barrier Islands from the Gulf of St. Lawrence to the Gulf of Mexico*. Academic, New York, pp. 1–27.
- Hayes, M.O., 1991. Geomorphology and sedimentation patterns of tidal inlets: a review. *Proc. Coastal Sediments '91*, ASCE, 1343–1355.
- Hume, T.M., Herdendorf, C.E., 1990. Morphologic and hydrologic characteristics of tidal inlets on a headland dominated, low littoral drift coast, Northeastern New Zealand. *Proc. Skagen Symposium (2–5 Sept. 1990)*. *J. Coastal Res.*, Spec. Issue 9, 527–563.
- Jarrett, J.T., 1976. Tidal prism-inlet area relationships. GITI Report, vol. 3. US Army Corps of Engineers, Waterways Experiment Station, Vicksburg, MS.
- Johnson, J.W., 1972. Tidal inlets on the California, Oregon, and Washington coasts. Tech. Rep. HEL 24-12, Hydraulic Eng. Lab., Univ. of Calif. at Berkeley, Berkeley, CA.
- Jones, C.P., Mehta, A.J., 1978. Ponce de Leon: glossary of inlets, Report No. 6. Florida Sea Grant College Report Number 23, UFL/COEL-78/014, U. of Florida, Coastal and Oceanographic Eng. Dept. Univ. of Florida, Gainesville, FL. 58 pp.
- Kragtwijk, N.G., 2001. Aggregated scale modeling of tidal inlets of the Wadden Sea: Morphological response to the closure of the Zuiderzee. M.Sc. thesis, Delft Univ. of Technol., Delft, The Netherlands.
- Kraus, N.C., 1998. Inlet cross-sectional area calculated by process-based model. *Proc. 26th Coastal Eng. Conf.*, ASCE, 3265–3278.
- Kraus, N.C., 2000. Reservoir model of ebb-tidal shoal evolution and sand bypassing. *J. Waterw., Port, Coastal, Ocean Eng.* 126 (3), 305–313.
- Larson, M., Kraus, N.C., 1989. SBEACH: numerical model for simulating storm-induced beach change. Report 1: empirical foundation and model development. Tech. Rep. CERC-89-9, U.S. Army Engineer Waterways Experiment Station, Coastal Eng. Res. Center, Vicksburg, MS.
- LeConte, L.J., 1905. Discussion on river and harbor outlets, “Notes on the improvement of river and harbor outlets in the United States,” Paper No. 1009, by D.A. Watts, *Trans. ASCE* 55, 306–308.
- Marino, J.N., Mehta, A.J., 1987. Inlet ebb shoals related to coastal parameters. *Proc. Coastal Sediments '87*, ASCE, 1608–1623.
- McClung, J.K., Douglass, S.L., 1999. Observing changes in an ebb-tidal shoal. *Proc. Coastal Sediments '99*, 734–749.
- Morang, A., 1999. Shinnecock Inlet, New York, Site Investigation Report 1: Morphology and historical behavior, Tech. Rep. CHL-98-32, U.S. Army Engineer Waterways Experiment Station, Coastal Eng. Res. Center, Vicksburg, MS.
- O’Brien, M.P., 1931. Estuary and tidal prisms related to entrance areas. *Civil Eng.* 1 (8), 738–739.

- O'Brien, M.P., 1969. Equilibrium flow areas of inlets on sandy coasts. *J. Waterw. Harb. Div.* 95 (WW1), 43–52.
- Parson, L.E., Lillycrop, W.J., McClung, J.K., 1999. Regional sediment management using high density Lidar data. *Proc. Coastal Sediments '99*, ASCE, 2445–2456.
- Renger, E., Partensky, H.W., 1980. Sedimentation processes in tidal channels and tidal basins caused by the artificial constructions. *Proc. 17th Coastal Eng. Conf.*, ASCE, 2481–2494.
- Riedel, H.P., Gourlay, M.R., 1980. Inlets/estuaries discharging into sheltered waters. *Proc. 17th Coastal Eng. Conf.*, ASCE, 2550–2562.
- Shigemura, T., 1981. Tidal prism-throat width relationships of the Bays of Japan. *Shore Beach* 49 (3), 34–39.
- Van Goor, M.A., 2001. Influence of relative sea level rise on coastal inlets and tidal basins: Are the Dutch Wadden capable of following the rising sea level? MSc thesis, Delft Univ. of Technol., Delft, The Netherlands.
- Vincent, C.L., Corson, W.D., 1981. Geometry of tidal inlets: empirical equations. *J. Waterw., Port, Coast., Ocean Div.*, ASCE 107 (1), 1–9.
- Walton, T.L., Adams, W.D., 1976. Capacity of inlet outer bars to store sand. *Proc. 15th Coastal Eng. Conf.*, ASCE, 1919–1937.